Available online at www.sciencedirect.com
SCIENCE DIRECT®
Environmental Modelling & Software 20 (2005) 623–638
Environmental Modelling & Software
www.elsevier.com/locate/envsoft

Prediction of personal exposure to contaminant sources in industrial buildings using a sub-zonal model

Zhengen Ren, John Stewart*

The QUESTOR Centre and The School of Computer Science, The Queen's University of Belfast, Belfast BT7 1NN, UK

Received 30 June 2003; received in revised form 8 September 2003; accepted 15 March 2004

Abstract

In this study the *COMIS with sub-zones* (COwZ) model was modified to allow predictions of personal exposure to contaminant sources in industrial buildings. A sub-zonal model of a person has been developed. Personal exposure resulting from various contaminant sources is simulated, taking both local variation in concentration and local influence of the occupant into account. The sub-zonal approach permits resolution of airflows, temperatures and pollutant concentrations within a room and throughout a whole building. COwZ incorporates zonal (sub-zonal) modelling within a conventional multizone model, offering advantages over multizone models but avoiding the greater difficulties associated with CFD modelling.

Numerical simulations made within a large, empty ventilated room using COwZ have been compared with published experimental measurements and results from CFD modelling studies. Comparisons have also been made with the results of CFD studies made when the room was occupied. The simulations show that the local impact of a person is significant in some cases and should be considered for the assessment of personal exposure.

Keywords: COwZ; Sub-zonal model; Numerical simulation; Modelling personal exposure

1. Introduction

The work described here is the initial stage of a project at the Queen's University's QUESTOR Centre[1] to develop a new occupational exposure model to predict employee exposure to air pollutants while they are at their place of work. The new program can also be used for other buildings. This paper concentrates on two significant aspects of the project: simulation of local air flow and pollutant dispersion; and, simulation of personal exposure.

We began by reviewing the development of models for indoor exposure which have been described by several authors (see, e.g., USEPA, 1992; Lioy, 1990; Brohus, 1997; Georgopoulos et al., 1997; IEH, 1999; Stewart, 2001).

Exposure models usually treat indoor microenvironments as well-mixed compartments where the concentration of a certain component is found by a simple mass balance (Maroni et al., 1995). When the air in a room is assumed to be fully mixed, the room-average concentration rather than a local value is used to predict exposure dose. This well-mixed assumption is usually inappropriate for large industrial buildings. Recently developed examples of this type of model are CPIEM (Koontz et al., 1998) and HAPEM4 (Rosenbaum, 2002).

Other indoor exposure models do not account for air flow fields within rooms, and users are required to supply air flow rates between rooms (see, e.g., RISK (Sparks, 1996), IAQX (Guo, 2000)). Some other models (such as EASE (HSE, 2000)) are knowledge-based systems derived from extensive data sets and make predictions based on matching release scenarios.

Rodes et al. (1991) summarised various measurements from the literature and stated that there may be considerable deviations between measurements using

* Corresponding author. Tel.: +44-28-90274037; fax: +44-28-90683890.
E-mail address: j.r.stewart@qub.ac.uk (J. Stewart).

[1] The Queen's University Environmental Science and Technology Research Centre is an industry-university co-operative research centre where the industrial members of the centre influence the content and direction of the research programme.

1364-8152/$ - see front matter © 2004 Elsevier Ltd. All rights reserved.
doi:10.1016/j.envsoft.2004.03.007

personal exposure monitors (PEM) and microenvironmental monitors (MEM). They found that typical ratios of PEM/MEM were from 1.58 to 13.40.

In practice, concentration gradients will occur, especially in large buildings. They may be expected to occur in the vicinity of contaminant sources and also when using displacement ventilation, where contaminant stratification with considerable gradients is utilised to improve ventilation effectiveness (Brohus and Nielsen, 1996).

CFD models are capable of predicting the air flow patterns and the distributions of pollutants arising from point or area sources at all positions over a finely-spaced grid filling the total volume of a room. CFD models have been used to predict general room airflow, inlet/outlet arrangements, occupant effects, displacement ventilation, and contaminant transport (Ren, 2002). But their application requires much specialised knowledge and sound engineering judgement. Some significant difficulties with CFD, especially when it is necessary to use three-dimensional analysis, include: that setting up the model, and identifying and specifying appropriate boundary conditions is difficult and time consuming; that the calculations are time consuming (especially for industrial buildings); that large amounts of computer memory are required (because of the restrictions on grid size) to enable adequate treatment of turbulence; and that they sometimes fail to converge to a solution. Furthermore, the large volume of the output requires considerable effort in post-processing and visualisation in order to understand the results.

The *COMIS with Sub-zones* (COwZ) model, recently developed by Ren and Stewart (Ren and Stewart, 2003; Stewart and Ren, 2003), is the culmination of a three year project at the Queen's University's QUESTOR Centre to develop a practical computer model which includes predictions of source emission rates, local concentrations and transport of pollutants inside large industrial buildings. It nests a zonal model within a multizone model (COMIS). This combines the ability to predict variations within rooms with the general whole-building modelling of a multizone model. COwZ offers advantages over multizone models but avoids many of the difficulties associated with CFD modelling.

Recently published work by Mora et al. (2003a,b) on the use of coarse grid CFD models demonstrates how these provide superior predictions of local air flows to those of zonal models. In their classification of zonal models, COwZ would be classed as a power law model with specific driven flows (PL-SDF). They show how PL-SDF models may be satisfactory for the SDF part of the flow regime, but tend to seriously underpredict flows in other regions where predictions rely mainly on the power law model. Their published results appear very promising and it will be interesting to see the extent to which they can succeed with more complex, three-dimensional room geometries and air flows, pollution sources, room occupants and in nesting their model within a multizone building model. Some of the advantages of coarse grid CFD would be lost if it becomes necessary to use a much finer grid to cope with more complex situations.

For occupational exposure modelling the approach we have taken is to modify COwZ to predict personal exposure to contaminant sources within buildings. A sub-zonal model of a person has been developed and implemented in COwZ to create a tool for assessing personal exposure. It is possible to simulate the characteristic flow phenomena observed close to a person and to simulate respiration and heat transfer between a room occupant and the environment. Personal exposure is estimated, taking both local concentration gradients and local influence of the person into account.

2. Sub-zonal exposure model

2.1. Description of COwZ

The transport and fate of environmental contaminants from their sources or points of formation in buildings will be highly dependent on effective modelling of contaminant emission and dispersion within and between the rooms. In such cases the critical room is sub-divided, using a Cartesian grid, into a relatively small number of discrete control volumes or cells (which we have called sub-zones). Within a sub-zone, temperature and concentration are assumed to be uniform. All other well-mixed rooms are treated as single zones.

The approach to the division of rooms into sub-zones employed here follows the techniques used in standalone zonal models (see, e.g., Inard et al., 1996; Musy et al., 1999). In the sub-divided rooms, two types of sub-zones are used: standard sub-zones and flow element (or mixed) sub-zones.

2.1.1. Standard sub-zones

Standard sub-zones are assumed to have a representative air temperature which does not differ markedly from their immediate neighbouring sub-zones. The important characteristic of these sub-zones is that flow velocities (and momentums) between them are small and primarily driven by pressure differences. Mass flows between adjacent sub-zones are calculated in different ways for horizontal and vertical interfaces.

For air flow across vertical interfaces,

$$m_{j,i} = C_{\mathrm{d}}\rho A|p_j - p_i|^n\left(\frac{p_j - p_i}{|p_j - p_i|}\right) \tag{1}$$

For air flow across horizontal interfaces,

$$m_{j,i} = C_d \rho A \left| (p_j - p_i) - \frac{g}{2}(\rho_i h_i + \rho_j h_j) \right|^n \left[\frac{(p_j - p_i) - g(\rho_i h_i + \rho_j h_j)/2}{|(p_j - p_i) - g(\rho_i h_i + \rho_j h_j)/2|} \right] \quad (2)$$

where $m_{j,i} \geq 0$ is the air mass flow rate leaving sub-zone j to sub-zone i, kg s^{-1}; C_d is discharge coefficient, m s^{-1} Pa^{-n}; A is a surface area of the common face between two sub-zones, m^2; ρ is air density, kg m^{-3}; p is sub-zone pressure, Pa; g is the acceleration due to gravity, m s^{-2}; and h is the height of the sub-zone, m.

2.1.2. Flow element sub-zones

Flow element sub-zones are used where local air flows are driven by ventilation inlets, fans, heaters or warm or cold room surfaces. In these cases the air flow velocities are better obtained using specific models to describe the driven flows (see Ren (2002) for many examples). We present here the equations for a two-dimensional ceiling jet used in the case studies presented later in the paper.

The jet height, $h(x)$, the maximum velocity, $u_m(x)$, the airflow rate, $q(x)$, and penetration length, l_{re} are (Rajaratnam, 1976; Heiselberg et al., 1998):

$$h(x) = 0.16x \quad (3)$$

$$u_m(x) = 3.5u_0\sqrt{\frac{b_0}{x}} \quad (4)$$

$$q(x) = 0.25q_0\sqrt{\frac{x}{b_0}} \quad (5)$$

$$l_{re} = 4.1H \quad (6)$$

where x is distance along the axis of the jet, m; q_0 is air flow rate at the inlet, kg s^{-1}; b_0 is the diffuser height, m; u_0 is the air flow velocity at the inlet, m s^{-1}; H is the height of a room, m.

Fig. 1 illustrates a ceiling jet occupying part of a flow element sub-zone. The air in the upper part of the flow element sub-zone is driven by the jet flow, while that in the lower part is not. Air flows in the lower part are calculated using the same methods as for standard sub-zones.

One area which still presents difficulties is the treatment required when two or more driven flows are expected to interact when their trajectories overlap. The outcome of such interactions presents a difficult problem for any modelling approach. It may be possible, in some cases, to repeat model runs with various arrangements of flow element sub-zone numbers and sizes to 'tune' the model to match measurements—but this approach has little practical value. In such circumstances we recommend reverting to the use of standard sub-zones beyond the region of interaction, accepting that this will tend to underestimate (or misrepresent) the magnitude and velocities of the air flows. If the interaction occurs in a region where velocities are relatively high it may be better to use a flow element sub-zone for the immediate area of the interaction.

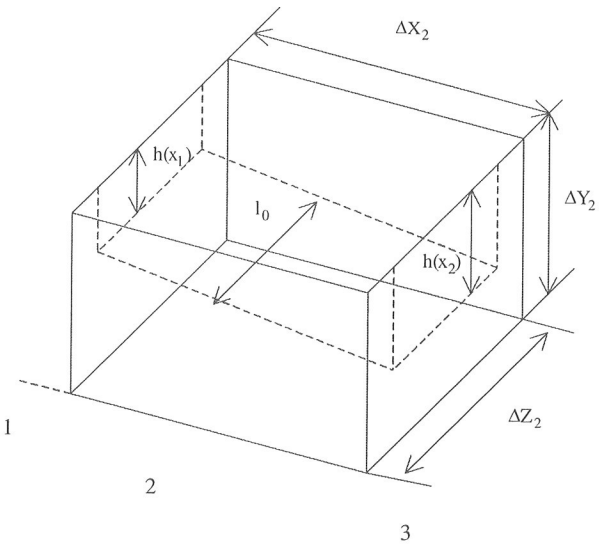

Fig. 1. Illustration of the volume occupied by the air flow generated by an inlet jet and contained within a flow element sub-zone.

2.1.3. Dividing a space into sub-zones

Usually, sub-zones are rectangular parallelepipeds set side by side. This simplifies the subdivision of rooms and the treatment of interfaces between sub-zones. But for non-rectangular rooms, the sub-zones near walls or corners may have other shapes.

It is necessary, at the outset, to decide on the appropriate number, size and shape of the sub-zones to be used. This requires prior consideration of the significant characteristics of the room and the resulting air flows which will be generated. The first task is to identify the flow drivers and their trajectories. As an example, for the ceiling jet, the penetration length is 4.1 times the room height and the depth of the jet, moving along the centre line in the direction of flow, is 0.16 times the distance from the inlet. These simple equations can be used to decide how many flow element sub-zones are needed along the path of the jet and how deep they should be to include all of the air flow associated with the jet.

In an empty room it is usually satisfactory to begin with sub-zones of 1–2.5 m in length and width, and 0.25–1.0 m high. Alternatively, use about 4–10 sub-zones in the vertical and 6–15 in the horizontal. The number, sizes and orientation are then modified to suit the features of the space being modelled. Where possible sub-zones are arranged to align with room features such

as doors, windows, flow obstructions, shapes and locations of flow drivers or any pollutant sources present. Setting up and running the model is simplified where a single sub-zone (or a small number) covers the feature. In regions where temperature or concentration gradients are high (near sources), and where it is desirable to resolve the distributions, more and smaller sub-zones may be used. For regions covered by standard sub-zones, accuracy does not increase markedly with the use of more and smaller sub-zones (see Ren, 2002; Ren and Stewart, 2003).

For thermal flow element sub-zones, where the temperature gradients are expected to be larger (e.g., a thermal plume or a thermal boundary near a hot wall surface), small sub-zones are needed; but large enough to contain the flow element. For a thermal boundary flow element sub-zone, we typically use between 0.1 and 0.5 m depth (from the warm surface). Such flow element sub-zones will, as noted in Section 2.1.2, require separate calculation of flow element air (the thermal boundary layer) and non-flow element air (that adjacent to the boundary layer flow). A combination of the flows arising in the boundary layer and outside the layer predict the total vertical flow for the sub-zone. A further paper describing the methodology in detail has been submitted for publication. For a thermal plume, the width of the sub-zone is determined by the width of the thermal plume (usually, 0.1–1.0 m). For a jet, the size of the sub-zones is determined by the local height/thickness of the jet flow (usually, 0.1–1.5 m).

For standard sub-zones, the temperature and concentration gradients are usually smaller (except where the sub-zones contain a pollutant source), the size is between 0.25 and 2.5 m. If a point pollutant source is present, smaller sub-zones may be appropriate.

2.1.4. Source emission modelling

When the network of a building with nodes (standard sub-zones, flow element sub-zones, undivided rooms, and the outside) and associated flow links has been entered, the solution of the non-linear system of equations for air mass and thermal energy balances (also included in COwZ) for each zone (or sub-zone) provides the pressure and temperature fields and air flow rates. When source emission rate is provided or source emission modelling has been included, pollutant concentration can also be calculated. Three types of source emission model (emission from liquid pools, wet paints, and gas and liquid release jets) have been implemented in COwZ (Ren, 2002).

2.1.5. Numerical methods

Full details of the numerical methods used in the program have been given in Ren (2002) and Stewart and Ren (2003). In summary, the Newton–Raphson method, and its modifications in appropriate cases, is used for the solution of the mass balance equations for the air flows. For the non-linear systems of equations for the thermal balances, we use Gaussian elimination with back substitution. Steady state pollutant transport equations are also solved using Gaussian elimination with back substitution, but for unsteady state cases a Gauss–Seidel iterative method is used.

2.2. Computer simulated person exposure model

The key task of exposure modelling is to predict the appropriate concentrations. In this new exposure model, exposure concentrations are addressed by combining COwZ and a computer simulated person exposure model. This section focuses on the development of such a model.

Brohus (1997) provides an extensive review of different models of people which have been developed for determination of personal exposure. The models may be divided into four different categories: heated cylinders; unheated, anatomically correct, small-scale models; heated, anatomically correct, full-scale models with respiration; and, the computer simulated person. The first three categories have been used in measurement research and the fourth is used in CFD studies.

The purpose of the models proposed in the following sections is to create a tool for assessing personal exposure when using a sub-zonal model. Our aim is to propose models which are both able to re-create the characteristic flow phenomena observed close to a person, and at the same time, have a minimised level of complexity that allows their use in practical engineering studies. The models must also simulate respiration and heat transfer between a human being and their environment.

2.2.1. Geometry and boundary conditions of models

In his CFD study, Brohus (1997) presented three models (shown in Fig. 2) to simulate air flow close to a person. These models did not include respiration. Our new models adopt this simplified rectangular geometry with the addition of heat transfer and respiration. The models are called Simplified Computer Simulated Persons, abbreviated to SCSP.

Table 1, adapted from Brohus (1997), summarises the geometry of a 1.7 m tall average-sized person. The aspect ratio of the width and the depth for the model are kept approximately constant and equal to two (Dunnett, 1994). The surface area is 1.62 m^2. Usually, the body surface area, A_{Du}, may be described as a function of weight (W_e) and height (H) (DuBois and DuBois, 1916),

$$A_{Du} = 0.20236 \cdot W_e^{0.425} \cdot H^{0.725} \quad (7)$$

The heat transfer boundary condition is chosen as a convective heat flux of 25 W m^{-2}, which corresponds

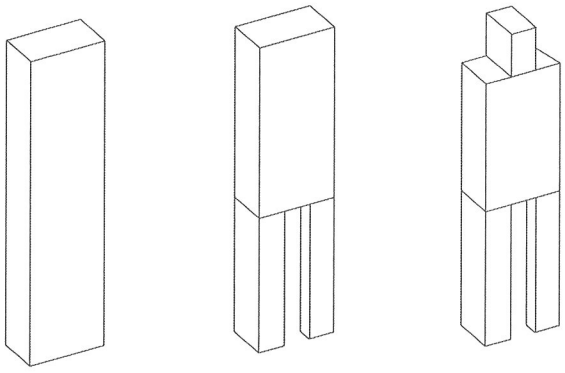

SCSP model 1 SCSP model 2 SCSP model 3

Fig. 2. Outline of the three Simple Computer Simulated Persons (SCSP) made in a rectangular geometry.

to the activity level of a person standing relaxed. The use of a heat flux boundary condition rather than a surface temperature avoids the more difficult task of modelling heat transfer by convection, radiation and conduction and the complications associated with sweating, diffusion through skin, respiratory moisture and carbon dioxide.

2.2.2. Respiration

For the assessment of personal exposure through inhalation, the exposure concentration and inhalation rate must be determined, which is affected by respiration.

The pulmonary ventilation rate is defined as the volume of air which is exhaled per minute. By definition, the pulmonary ventilation equals the frequency of respiration multiplied by the mean expired volume (Åstrand and Rodahl, 1986):

$$V_{res} = f_{res} \cdot V_T \tag{8}$$

Table 2, adapted from Asmussen and Nilsen (1989), shows examples of typical levels of the three parameters for different activity levels.

Any inhaled contaminants obviously come from contaminated air in the breathing zone close to the mouth and nose. To examine from what distance or volume the air is inhaled, Brohus (1997) presented a simplified approach, which is used where the nose (or mouth) is treated as an exhaust opening with a total area of 1.3 cm^2 corresponding to the two nostrils of a person (see Fig. 3). We use this method to calculate the minimum size for a sub-zone containing the person's mouth.

Table 1
Geometry of the three Simple Computer Simulated Persons (adapted from Brohus, 1997)

Part	SCSP model 1	SCSP model 2	SCSP model 3
Torso	1.7×0.3×0.16216	0.9×0.3×0.13803	0.67×0.3×0.14429
Leg	–	0.8×0.105×0.13803	0.8×0.105×0.14429
Head	–	–	0.23×0.13×0.18

Length×width×depth (m). Convective heat flux: 25 W m^{-2}. Surface area: 1.62 m^2. The surface area is the 'exposed area', i.e., the part of the surface in contact with the surrounding air (this implies that the area in contact with the floor is not included).

Table 2
Examples of expired volume, frequency of respiration and pulmonary ventilation for different activity levels (adapted from Asmussen and Nielsen, 1989)

Activity level	Expired volume V_T (l)	Frequency f_{res} (min^{-1})	Pulmonary ventilation V_{res} (l min^{-1})
Rest	0.5	12	6
Moderate work	~2.5	12	30
Maximal work	~3.0	30–40	90–120

The velocity, u_r, at a distance r from the opening may be found by assuming inhalation from a hemispherical surface (Brohus, 1997),

$$u_r = \frac{m_r}{A_{Ex} + 2\pi r^2} \tag{9}$$

where A_{Ex} is the opening area (nostril area) and m_r is the volumetric flow rate.

From Table 2 the pulmonary ventilation for a person at moderate work is 30 l min^{-1}. The inhalation, however, does not take place continuously but intermittently at approximately 12 times per minute. If the inhalation takes place half the time, $m_r = 60$ l min^{-1}. Brohus chose a capture velocity, $u_r = 0.25$ m s^{-1} and a nostril area, $A_{Ex} = 1.3$ cm^2 which yields a radius, $r = 2.5$ cm. This corresponds to a hemispheric volume of approximately 30 cm^3. Eq. (9) links capture velocity to a capture radius and capture volume. The air within the capture volume will be inhaled.

For a person at rest, $r = 1$ cm, and the hemispheric volume is approximately 2 cm^3, i.e., in both cases relatively small volumes and small distances from the nose/mouth are obtained.

This analysis suggests that the personal exposure for the SCSP may be simulated as the mean concentration of a volume between 2 cm^3 and 30 cm^3 adjacent to the surface at the breathing zone height, i.e., 1.5 m above the floor for a standing average sized person. This volume depends on the choice of capture velocity; here Brohus has chosen 0.25 m s^{-1}.

2.2.3. Subdivision of zones near a person

We have described how sub-zone sizes are chosen for standard and flow element sub-zones and have summarised Brohus' analysis of the air volume captured during inhalation. Now we consider the implications for setting up sub-zones near a room occupant. Heat transfer between a person and their surroundings and

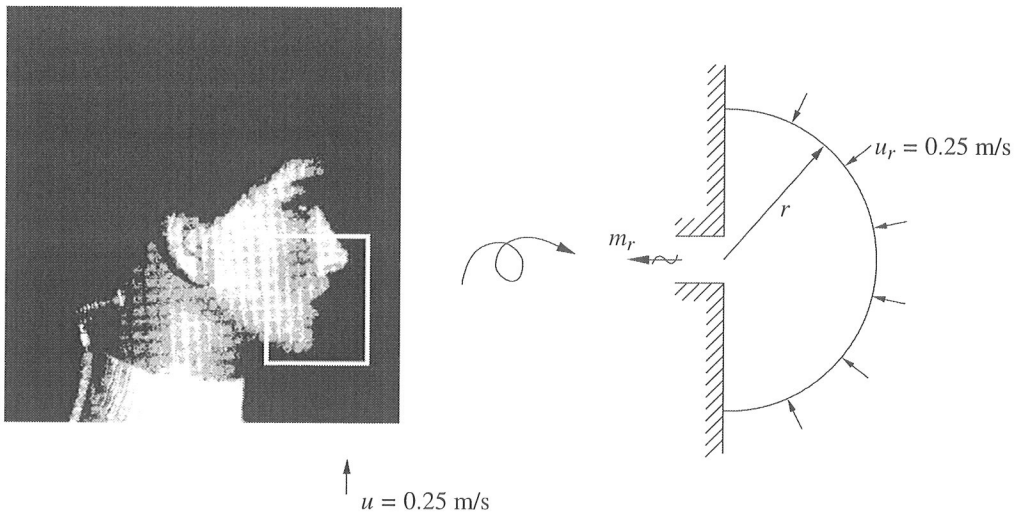

Fig. 3. Simplified model of inhalation to estimate from what volume the air is drawn. The area of the 'exhaust opening' is 1.3 cm^2 and the necessary capture velocity is assumed to be 0.25 m s^{-1} (adapted from Brohus, 1997).

via respiration will have significant influence on local airflows and subsequent personal exposure. The choice of location and size of sub-zones near a person should enable this influence to be modelled.

Fig. 4 illustrates a very simple geometry, but one which is suitable for the case studies described in this paper. The sub-zone surfaces adjacent to the occupant are 'non flow', which takes care of the obstruction effect on room air flows. Otherwise, these are simple standard sub-zones. The heat input from the occupant's body is relatively small and no special treatment of flow element/non-flow element air has been used. All the sub-zones are assigned a heat input in proportion to their area of contact with the body. The heat transferred is assumed to change the temperature of all the air in the adjacent sub-zone. In this simple model, except for the region near the head, there is no advantage to be gained from the use of a larger number of smaller sub-zones close to the occupant. Near the head of the occupant we have used smaller sub-zones to improve the resolution of the human exposure concentration (by inhalation).

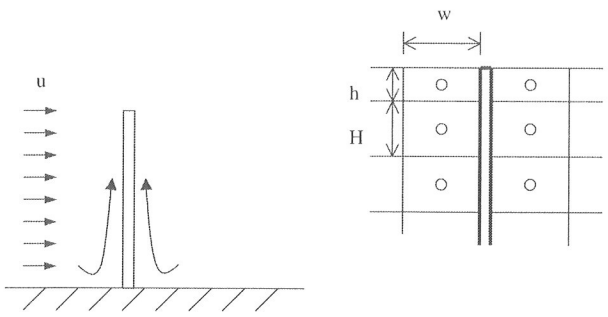

Fig. 4. The sub-zone layout around the most basic upright SCSP.

As described in the previous sub-section, the radius of the breathing hemisphere (r) is 1–2.5 cm, and the dimension of the head is 0.23×0.13×0.18 (m) (see Table 1). Here we have set the height of the breathing sub-zone to 0.23 m, the width to 0.1 m, and the depth to 0.18 m. The sub-zone volume is just over 4 l, substantially more than the hemispheric volume calculated in the previous section which we have interpreted as a minimum. The tidal volume of the lungs varies from 0.5 to 3 l (Table 2). For other sub-zones, where heat from the body causes a rising flow, the height of the sub-zones can be larger, for example, 0.5 m.

Although the allocation of sub-zones is rather basic, even this simple approach will accommodate variation in heat transfer rates from different parts of the body and heat exchange associated with respiration—though neither of these are required for the case studies described below.

3. Exposure analysis and assessment

3.1. Introduction

The transport and fate of environmental contaminants from their sources or points of formation in the environment to the point of their biological effect can be represented in terms of a continuous exposure sequence (Lioy, 1990). In general, contaminants may be taken up by the human body via one or more of the three common routes of inhalation, dermal absorption, and ingestion.

Depending on the purpose for which an exposure assessment will be used, the numerical output of an exposure assessment may be an estimate of either exposure or dose. If exposure assessments are carried out

as part of a risk assessment that uses a dose–response relationship, the output usually includes an estimate of dose (NRC (National Research Council), 1983). Other risk assessments, for example many of those done as part of epidemiological studies, use exposure–response relationships, and may characterise risk without the intermediate step of estimating dose. Our new model includes estimations of exposure and dose, which are described below.

3.2. Exposure

The potential for exposure arises when some chemical contaminant comes into contact with the outer surface of a person. Most of the time, the chemical is contained in air, water, soil, a product or a transport or carrier medium; the chemical concentration at the point of contact is the exposure concentration. Exposure over a period of time can be represented by a time-dependent profile of the exposure concentration, which is expressed as,

$$E = \int_{t_1}^{t_2} C(t)\mathrm{d}t \tag{10}$$

where E is the magnitude of exposure, $C(t)$ is the exposure concentration as a function of time, and t is time.

Eq. (10) can also be expressed in discrete form as a summation of exposure received during various events i:

$$E = \sum_i C_i ED_i \tag{11}$$

where ED is the exposure duration, $t_{i+1} - t_i$.

3.3. Dose

The dose is defined as the quantity of some chemical entering the body over a period of time. The process of a chemical entering the body can be described in two steps: firstly contact (exposure), and secondly actual entry (crossing the boundary). A chemical crossing the boundary from outside to inside the body undergoes two major processes: intake and uptake. Dose for the two processes is described below.

3.3.1. Applied dose and potential dose

Applied dose is the amount of a chemical at the absorption barrier (skin, lung, gastrointestinal tract) available for absorption. A relationship between applied dose and internal dose is useful. However, it is very difficult to measure the applied dose directly, as many of the absorption barriers are internal to the body and are not localised in such a way as to make measurement easy. The concept of potential dose is used as an approximation of applied dose (Lioy, 1990; NRC (National Research Council), 1990).

Potential dose is simply the amount of the chemical ingested, inhaled, or in material applied to the skin. The general equation for potential dose for intake processes, e.g., inhalation and ingestion, is simply the integration of the chemical intake rate:

$$D_{\mathrm{pot}} = \int_{t_1}^{t_2} C(t)IR(t)\mathrm{d}t \tag{12}$$

where D_{pot} is the potential dose and $IR(t)$ is the inhalation or ingestion rate.

Eq. (12) can also be expressed in discrete form as a summation of the doses received during various events i:

$$D_{\mathrm{pot}} = \sum_i C_i \cdot IR_i \cdot ED_i \tag{13}$$

3.3.2. Internal dose (especially via respiratory and oral routes)

Chemicals in air, food, or drinking water normally enter the body through intake processes, then are subsequently absorbed through internal uptake processes in the lung or gastrointestinal tract. Sometimes it is necessary to estimate resulting internal dose, D_{int}, after intake. Assuming potential dose and applied dose are approximately equal, the internal dose after intake can be estimated by Eq. (14):

$$\begin{aligned} D_{\mathrm{int}} &= D_{\mathrm{app}} \cdot AF \cong D_{\mathrm{pot}} \cdot AF \\ &= \sum_i C_i \cdot IR \cdot ED_i \cdot AF \end{aligned} \tag{14}$$

where AF is the absorption fraction in units of mass absorbed/mass applied (dimensionless).

4. Estimation of personal exposure using COwZ

This section presents simulations of personal exposure to contaminant sources located in a mixing ventilated room where the entire flow field in the room is modelled.

4.1. Geometry and boundary conditions

We have chosen to perform the simulations on a well-documented test case in order to facilitate comparisons between the new program simulations and measurements and CFD simulation found in the literature. The test case is described by Nielsen (1990), and it has been used as part of the International Energy Agency, Annex 20 work.

The mixing ventilated room is shown in Fig. 5 where the co-ordinate system is defined and the dimensions are given.

Three different cases are examined: Case 1, an empty room; Case 2, SCSP model 1 located at $(x, z) = (3, 0)$;

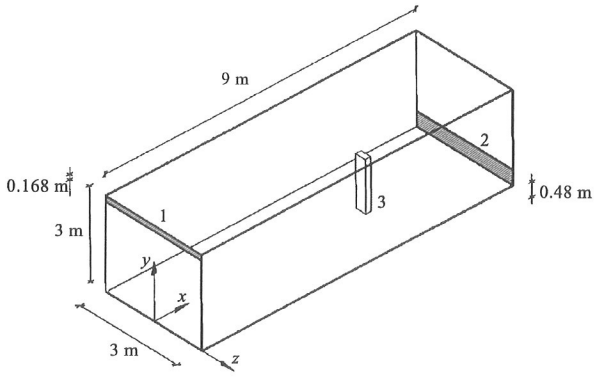

Fig. 5. Geometry of the ventilated room used in the case studies. The air is supplied at the inlet (1) located close to the ceiling, and is exhausted at the return opening (2) located close to the floor at the opposite end. The SCSP model 1 (3) is located in the symmetry plane, $z = 0$ m (adapted from Brohus, 1997).

and Case 3, SCSP model 1 located at $(x, z) = (6, 0)$. For Case 1 the empty room is symmetric and simulated in two dimensions (1 sub-zone in the z direction). Cases 2 and 3 have been modelled in three dimensions as the rising warm air flow from the occupant, located at the room mid-plane, is expected to interact with the horizontal jet flow from the inlet. The flows are expected to be symmetric about the mid-plane so only one half of the room need be modelled. Three sub-zones are used in the z direction.

The inlet conditions for the test case are as described by Nielsen (1990). The inlet velocity is 0.455 m s^{-1}, which corresponds to an air change rate of 10 h^{-1}. The supply air temperature is 21 °C. In Case 1 the flow is isothermal, and in Case 2 and Case 3 the only heat source is the SCSP with a surface heat flux of 25 W m^{-2}. The walls are adiabatic. The air inlet jet is a room-wide opening at $x = 0$, at the top of the wall. The outlet is a room-wide opening at $x = 9$ and the bottom of the wall.

4.2. Simulation of the flow field

Fig. 6 shows the flow field in the room for the three different cases. The CFD simulations by Brohus (1997) are shown in Fig. 7.

For the empty room, the important driving flow is the inlet jet. The air flow pattern is expected to be uniform in the z direction and the room is modelled in two dimensions. We have used six evenly sized sub-zones of 1.5 m in the horizontal (x) direction. The depths of the flow element sub-zones for the jet are determined from Eq. (3) (0.24, 0.48, 0.72, 0.96 and 1.2 m) and the jet penetrates to the far wall of the room. The heights of the remaining sub-zones are set to 0.4 m or 0.5 m (lowest sub-zone layer to incorporate the exit vent).

The other two cases are modelled in three dimensions. The room is 3 m wide and, in these simple cases, the flow regime will be symmetrical about the centre-plane. Thus, effort can be saved by modelling one half of the room. The space was divided into three sub-zone columns 0.5 m wide in the z direction. We can anticipate that upward warm air flow from the occupant will interact with the jet flow across the ceiling. Without prior knowledge of the resulting flow pattern we simply assume the flow beyond the interaction region can no longer be described by Eqs. (3)–(6) and therefore use standard rather than flow element sub-zones for this region. For this reason, beyond the occupant location, the heights of the upper layer of sub-zones no longer 'step down' as they do when Eq. (3) is used.

Broadly speaking, COwZ provides results that compare reasonably well with the CFD computed results described by Brohus (1997), which were reported to agree with the measurements of Nielsen (1990) very well, although, for Cases 2 and 3, the CFD model captures the dead flow field at the right part of the room more markedly than COwZ.

In the empty room (Case 1), a typical recirculating flow field is found. There is a relatively high velocity flow in the x direction near ceiling, the flow field expands vertically with distance from the inlet. There is a substantial downwards flow at the far end wall which the CFD shows dividing near the exit to form a weaker recirculating flow along the floor. There is a low-flow zone near the centre of the room. The flow pattern is dominated by the inlet jet. These features are all observed in the output from COwZ as illustrated in Fig. 8. Note that, as mentioned in the introduction, air velocities are modelled quite accurately in the jet region but are underestimated in the recirculation region in lower half of the room.

When a person, represented by a SCSP, is located in the room (Case 2 and Case 3) the flow field is significantly affected both near to the person and throughout the whole room. The SCSP generates a strong upward-moving thermal plume which then interacts with the inlet jet near the ceiling. A low-flow recirculation is generated downwind of the interaction zone. The inlet jet is partly diverted in the z direction to either side of the rising warm air flow. The COwZ model results (bearing in mind Case 1 has one cell in the z direction while Cases 2 and 3 have 3 cells to simulate one half of the room) also capture these modified flow regimes except that the low-flow recirculation where the thermal plume interacts with the inlet jet is not so well resolved.

4.3. Simulation of personal exposure

This section will present simulation of personal exposure to a planar source in the shape of the floor as well as point sources at different locations in the room. The simulations were performed for the empty room and

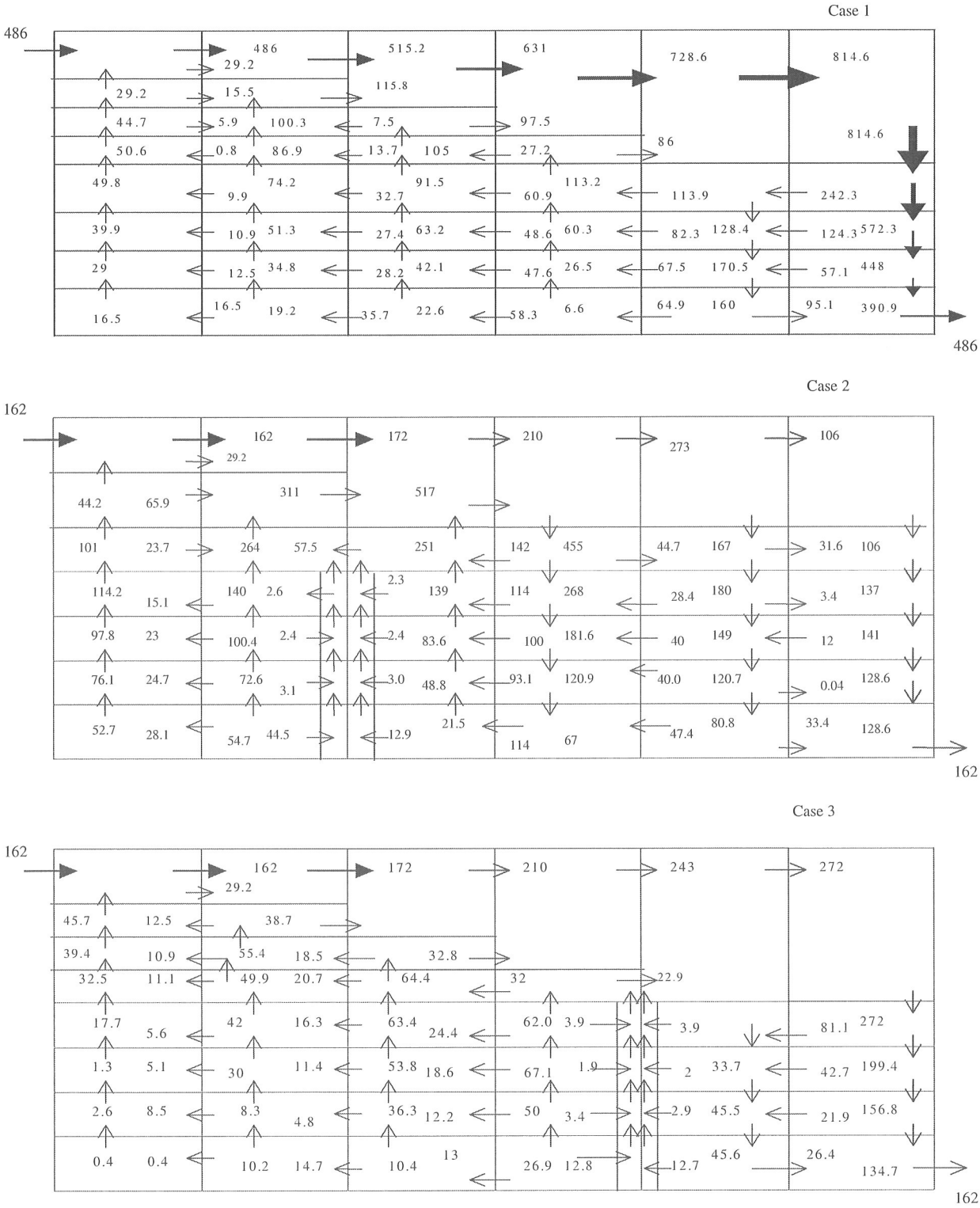

Fig. 6. Air flow rate (kg h^{-1}) for Cases 1, 2 and 3 using COwZ in the plane $z = 0$ m (vertical symmetry plane).

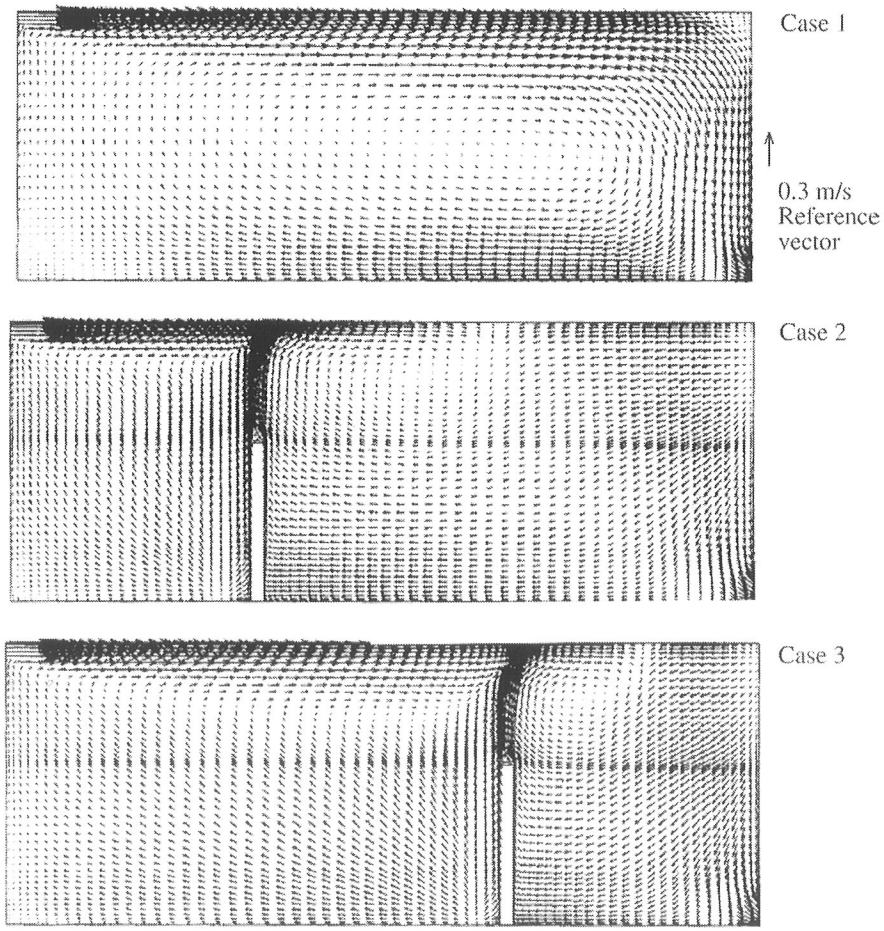

Fig. 7. CFD vector plot, in the plane $z = 0$ m, for Cases 1, 2 and 3 reported by Brohus (1997).

two different locations of the SCSP. In all cases the personal exposure of the SCSP corresponds to the contaminant concentration in the nearest sub-zone to the mouth and nose at a height of 1.5 m.

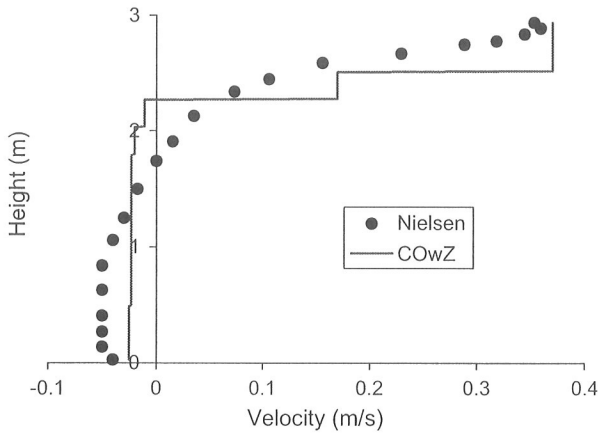

Fig. 8. Vertical velocity profile at $(x, z) = (3, 0)$ showing a comparison between COwZ and Nielsen's (1990) measurements.

4.3.1. Planar contaminant source

Fig. 9, adapted from Nielsen (1981), shows the comparison of concentration distribution from COwZ and Nielsen's measurements and his numerical calculation at the height $0.25H$ through the occupied zone of the empty room (Case 1). A constant contaminant source is assumed along the whole floor surface. The COwZ model concentration distribution is close to the experimental results.

A comparison between COwZ and CFD (Nielsen, 1981) for the whole room and Case 1 is shown in Fig. 10. The contours from COwZ were produced using the SURFER® program to interpolate linearly between the predicted concentrations located at the centre of each sub-zone. A very good agreement is found with contaminant accumulating in the poorly ventilated area near $x = 0$ and $y = 0$.

Fig. 11 shows how a person in shape of the SCSP located in the room (Cases 2 and 3) modifies the contaminant distribution. These cases were also simulated by Brohus (1997) using a three-dimensional CFD calculation, and a good agreement is found.

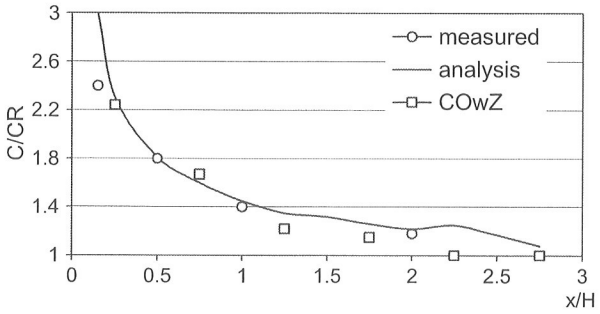

Fig. 9. Comparison of dimensionless concentration from COwZ, measurement and numerical calculation (adapted from Nielsen, 1981) at a height $0.25H$ through the occupied zone of the room. C_R is the concentration in the return opening.

If the room air was perfectly mixed, the dimensionless contaminant concentration (Cp) as well as the personal exposure (Ce) would equal 1 in all cases shown in Figs. 10 and 11. However, the simulations clearly show the significant concentration gradients generated close to the contaminant source (the floor, particularly at the left corner) and also close to the SCSP in Case 2 (Case 2 and Case 3 reported by Brohus).

The concentration gradients result in a dimensionless exposure ranging from 1.0 to 1.9, dependent on SCSP location. Changing the orientation of the SCSP (to face right or left in the diagrams) changes the exposure from 1.3 to 1.9 in Case 2. Brohus (1997) reports corresponding values of 1.2 and 2.0.

4.3.2. Passive point concentration source

A passive point contaminant source is defined as a pollutant source without any significant initial momentum or buoyancy, i.e., the pollution is supplied with a very low velocity at room air temperature and at room air density. An example would be emissions from building materials and other 'cold' sources. A neutral density mixture of nitrous oxide (N_2O) and helium (He) was used for this study.

For these tests a passive point source was positioned 1 m from the floor and on the room mid-plane. For Case 2, where the SCSP is at $x = 3$ m, the source is at $x = 2$ and then $x = 4$ m. For Case 3, where the SCSP is at $x = 6$ m, the source is at $x = 5$ and then $x = 7$ m.

Figs. 12 and 13 show the relevant isoconcentration plots. These situations were also modelled by Brohus (1997) using a three-dimensional CFD simulation. For Case 2 both models predict dimensionless concentrations ranging from 1.0 to 6.0, but for Case 3 it is 1.0 to 5.0 from COwZ and 1.0 to 6.0 from CFD (Brohus, 1997).

The distribution of pollutants results in a dimensionless exposure ranging from 1.0 to 3.0 (1.1–4.9 reported by Brohus), highly dependent on source location and SCSP location and orientation. With the SCSP at $x = 3$ m and with the point source at $x = 4$ m, the predicted exposures are 1.7 when facing left and 3.0 when facing right. Brohus reported values of 1.6 and 4.9 for these cases. This obviously demonstrates the importance of including the local influence of a person and their orientation when exposure is modelled.

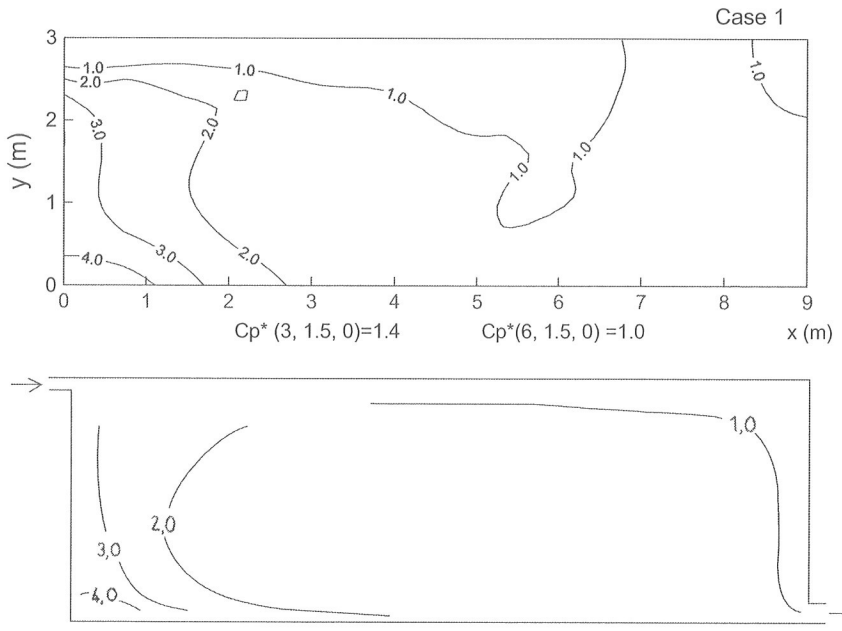

Fig. 10. Comparison of computed dimensionless concentration in the vertical symmetry plane ($z = 0$ m) for Case 1 using COwZ (upper figure) and measurements reported by Nielsen (1990) (lower figure). The floor is a planar source. The dimensionless concentration, $Cp^* = C/C_R$.

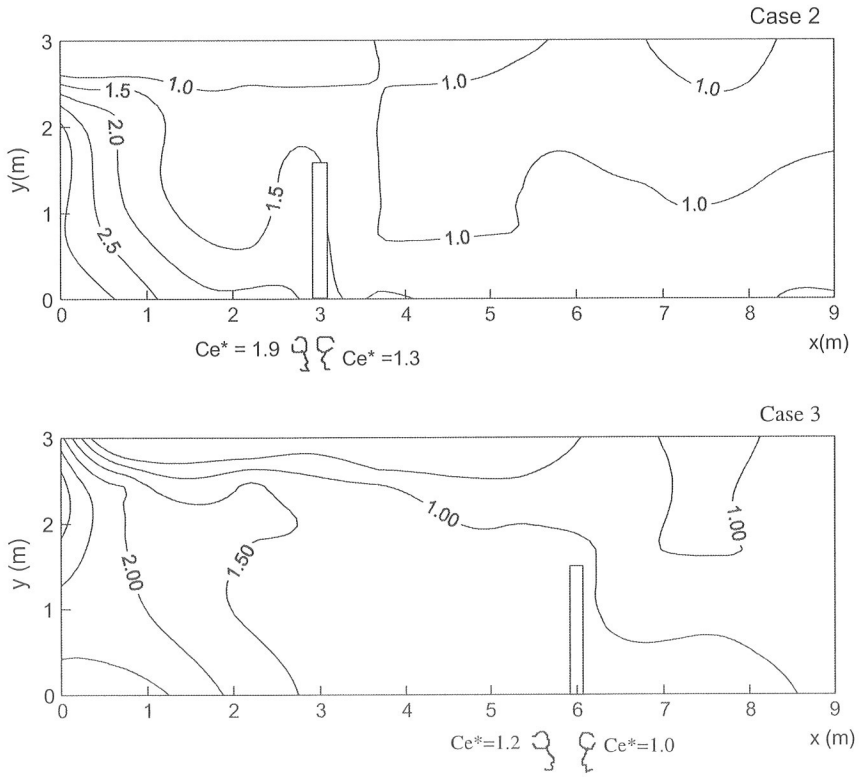

Fig. 11. Dimensionless contaminant concentration distribution in the vertical symmetry plane ($z = 0$ m) for Cases 2 and 3 using COwZ. The floor is a planar source. The dimensionless exposure concentration, $Ce^* = C/C_R$.

4.4. Analysis and assessment of inhaled dose

This section presents an assessment of the inhaled dose when a person occupies the room with a planar source in the shape of the floor as well as point sources at different locations. The assessment was performed for two different locations of the SCSP (Case 2 and Case 3). In all cases the contaminant source, a neutral density mixture of nitrous oxide (N_2O) and helium (He), was a continuously injected gas at 0.135 mg s^{-1}.

For the planar source in the shape of the floor, the inhaled dose over 8 h is shown in Fig. 14 for an occupant doing moderate work (breathing rate at 30 l m^{-1}, see Table 2) at the locations, $(x, z) = (3, 0)$, Case 2, and $(x, z) = (6, 0)$, Case 3. See Table 3 for key. For different locations of point sources, the results are shown in Figs. 15 and 16 for Case 2 and Case 3, respectively.

Fig. 14 shows that, over an 8-h moderate work period, the occupant located at $(x, z) = (3, 0)$ and facing left (D21, in Fig. 14) inhaled nearly twice the gaseous pollutants than if he worked at $(x, z) = (6, 0)$ and faced right (D32, in Fig. 14). Over 8 h at location $(x, z) = (3, 0)$, the inhaled dose was 22.5 or 32.8 mg depending on the direction faced. At location $(x, z) = (6, 0)$ the inhaled dose was 17.3 or 20.7 mg depending on direction faced.

For the point source cases, the highest exposure occurred when the pollutant source was upwind (local flow direction) and the occupant faced towards it. For Case 2 this corresponded to the point source at location $(x, y, z) = (4, 1, 0)$ and the occupant facing right (see Fig. 6 for the airflow direction). The inhaled dose was 51.8 mg over 8 h moderate work (D24, in Fig. 15), while it was 17.3 mg when the point source was located downwind and the person faced away from it (D22, in Fig. 15). For Case 3, worst case was when the point source was at $(x, y, z) = (7, 1, 0)$ and the occupant faced right. The inhaled dose was 51.8 mg over 8 h moderate work (D34, in Fig. 16), while it was only 19.0 mg when the point source was located downwind of the occupant who faced away from it (D32, in Fig. 16).

We have shown how personal exposure within the ventilated room is determined by location and orientation of both occupant and pollutant source. Inhaled dose is also affected by the degree of activity (rest, moderate work or heavy work). Considering the results generated from these case studies, the minimum inhaled dose over 8 h, where the occupant is resting, is 17.3 mg while the maximum inhaled dose, where the occupant

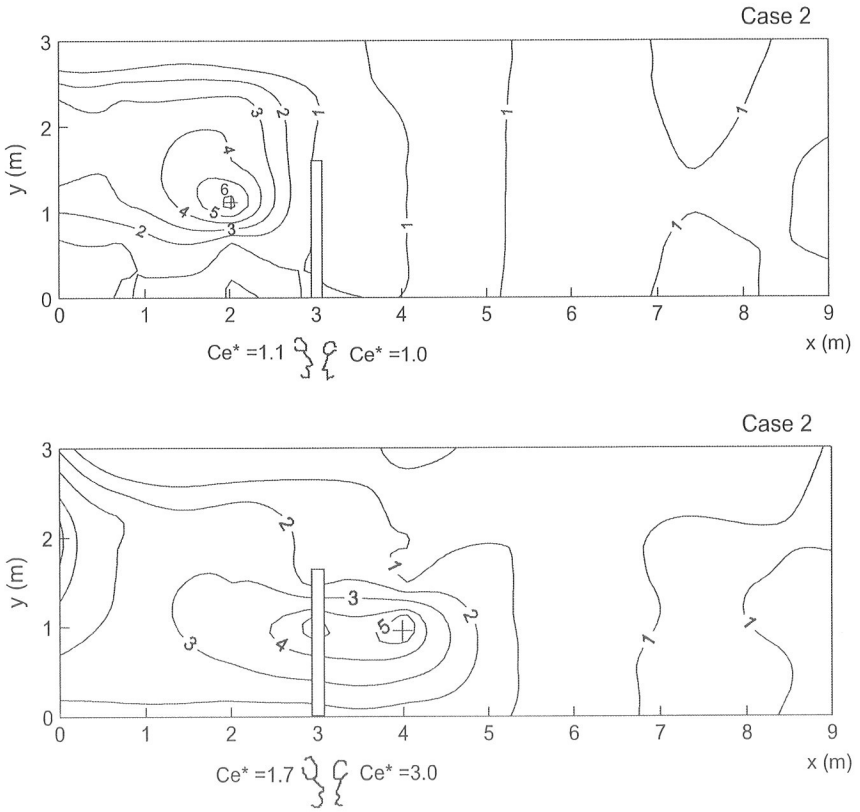

Fig. 12. Dimensionless isoconcentration plot from the vertical symmetry plane ($z = 0$ m) for two different locations of the passive point concentration source in the room, Case 2. Top: source location $(x, y, z) = (2, 1, 0)$. Bottom: source location $(x, y, z) = (4, 1, 0)$. The dimensionless exposure concentration, Ce^*, is given for two different orientations of the person in each case.

does heavy work and faces a point source at 1 m distance, is 181.4 mg—a difference of more than a factor of ten.

5. Program details

The COwZ program was developed at the QUESTOR Centre and the School of Computer Science at Queen's University, Belfast by Zhengen Ren and John Stewart. It adds substantially to the basic COMIS multizone modelling program (Feustel and Rayner-Hoosen, 1990). Like COMIS, it is written in FORTRAN 77 with some use of FORTRAN 90. It was developed using Digital Visual Fortran v6 and may be compiled to execute on PCs or Unix machines. Input and output are by way of standard ASCII text files. There is no graphical user interface. We are developing an 'intelligent assistant' program to help with the creation of input files.

The minimum hardware requirement to execute the program is a Pentium II processor, Microsoft Windows NT or Windows 95, 16 MB of RAM and 10 MB of hard disk space. However, the program will execute much more quickly, especially for larger problems, with more memory and faster processors.

The source and executable code for COwZ is available, without charge to other researchers, from John Stewart by e-mail at j.r.stewart@qub.ac.uk or check for details on our web site at http://www.qub.ac.uk/qc/webpages/whatwedo/researchgroups/enviromentalmodelling/ia/.

6. Conclusion

In this study personal exposure to contaminant sources in a ventilated room is examined using a modified version of the COwZ model and combining it with a simple sub-zonal model of a person. The capability to resolve variations in airflow, temperature and pollutant concentration within rooms makes it possible to estimate personal exposure in large buildings. The local influence of the person on the flow field is included both for convective heat transfer and effects as an obstacle to the flow field. Results from the new program have been compared with published measurements and CFD models. The comparison indicates that

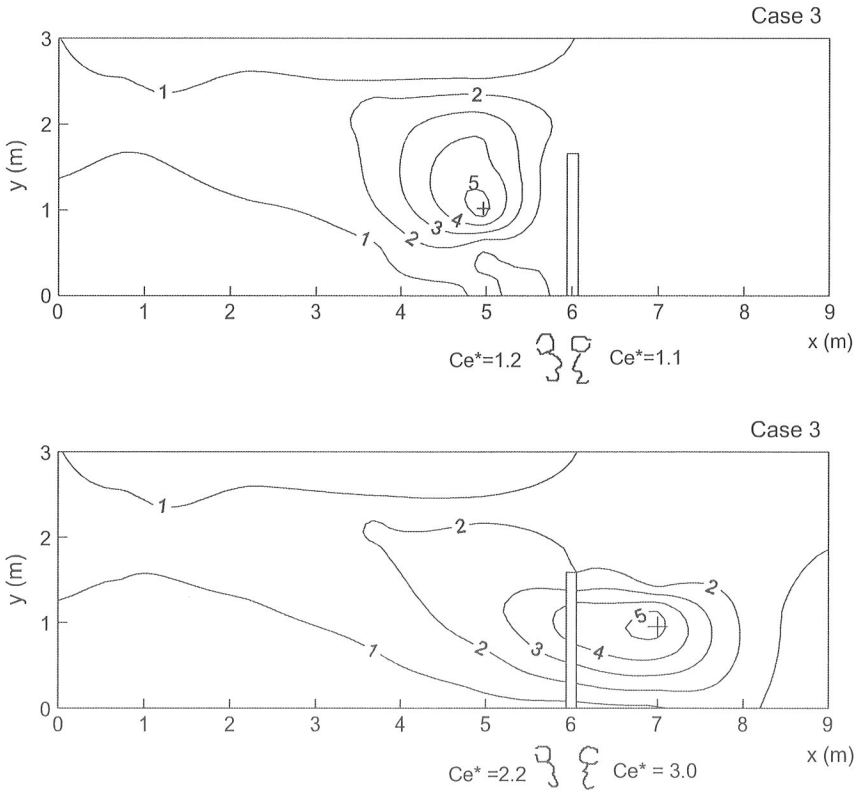

Fig. 13. Dimensionless isoconcentration plot from the vertical symmetry plane ($z = 0$ m) for two different locations of the passive point concentration source in the room, Case 3. Top: source location $(x, y, z) = (5, 1, 0)$. Bottom: source location $(x, y, z) = (7, 1, 0)$.

this new program is an effective model for predicting air flow and personal exposure within buildings. For the assessment of inhaled dose, personal activity level is also considered.

The results illustrate the important influence of location and orientation of a person and that the local impact of the person and their activity should be considered in the exposure assessment.

Compared to conventional CFD, COwZ can be used to make approximate, but useful, predictions of air flows and concentration distributions within buildings at zonal level requiring less time and computer memory. The user requires a different expertise from that needed for CFD work.

COwZ combines the features of zonal and multizonal modelling. A sub-zonal model has been developed and combined with COwZ to account for the effects of occupants on air flows and personal exposure. It appears that no other currently available zonal model provides this combination of features (zonal model with multizonal modelling and sub-zonal modelling of an occupant).

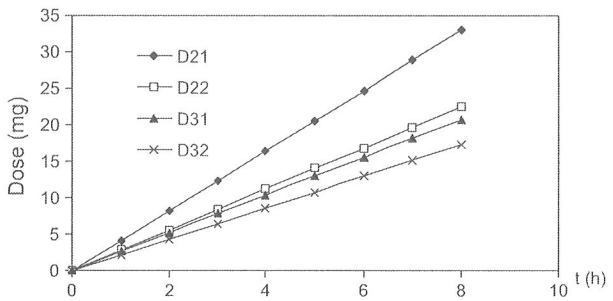

Fig. 14. Predicted inhaled dose for an occupant doing moderate work with a planar source in the shape of the floor.

Table 3
Key for position of occupant, direction facing and location of point source (Figs. 15 and 16 only) for Figs. 14–16

Key	SCSP (x, z)	Facing left or right	Point source (Figs. 15 and 16) (x, y, z)
D21	3,0	L	2,1,0
D22	3,0	R	2,1,0
D23	3,0	L	4,1,0
D24	3,0	R	4,1,0
D31	6,0	L	5,1,0
D32	6,0	R	5,1,0
D33	6,0	L	7,1,0
D34	6,0	R	7,1,0

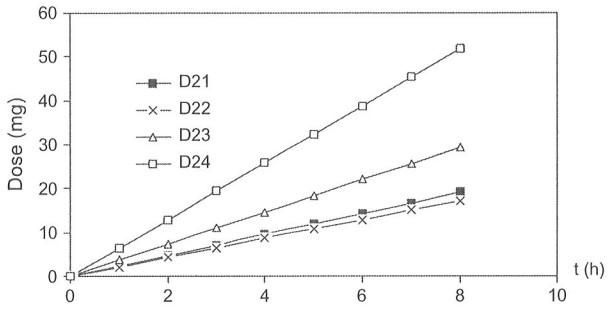

Fig. 15. Predicted inhaled dose for an occupant at location $(x, z) = (3, 0)$ (Case 2) and doing moderate work with a point source at $(x, y, z) = (2, 1, 0)$ and $(x, y, z) = (4, 1, 0)$. See Table 3 for key.

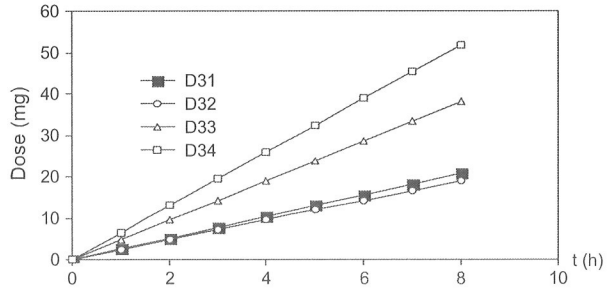

Fig. 16. Predicted inhaled dose for an occupant at location $(x, z) = (6, 0)$ (Case 3) and doing moderate work with a point source at $(x, y, z) = (5, 1, 0)$ and $(x, y, z) = (7, 1, 0)$. See Table 3 for key.

Acknowledgements

This project and COwZ are both funded by a grant from The Queen's University Environmental Science and Technology Research (QUESTOR) Centre.

References

Asmussen, E., Nielsen, M., 1989. Lærebog i menneskets fysiologi. Akademisk. Akademisk Forlag.

Åstrand, P.O., Rodahl, K., 1986. Textbook of Work Physiology – Physiological Bases of Exercise. McGraw-Hill, ISBN 0-07-100114-X.

Brohus, H., 1997. Personal exposure to contaminant sources in ventilated rooms, PhD thesis. Aalborg University, Denmark. ISSN 0902-7953 R9741.

Brohus, H., Nielsen, P.V., 1996. Personal exposure in displacement ventilated rooms. Indoor Air 6 (3), 157–167.

DuBois, D., DuBois, E.F., 1916. A formula to estimate approximate surface area, if height and weight are known. Archives of Internal Medicine 17, 863–871.

Dunnett, S.J., 1994. A numerical study of the factors affecting worker exposure to contaminants. Journal of Aerosol Science 25 (Suppl. 1).

Feustel, H.E., Rayner-Hoosen, A., 1990. COMIS Fundamentals. LBNL-28560, Lawrence Berkeley National Laboratory Report, Berkeley, CA.

Georgopoulos, P.G., Walia, A., Roy, A., Lioy, P.J., 1997. Integrated exposure and dose modelling and analysis. Environmental Science and Technology 31 (1), 17–27.

Guo, Z., 2000. Development of a Windows-based indoor air quality simulation software package. Environmental Modelling and Software 5, 403–410.

Heiselberg, P., Murakami, S., Roulet, C. (Eds.), 1998. Ventilation of large spaces in buildings: analysis and prediction techniques. Energy Conservation in Buildings and Community Systems. Annex 26: Energy Efficient Ventilation of Large Enclosures. International Energy Agency.

HSE (The Health and Safety Executive), 2000. The assessment of workplace exposure to substances hazardous to health: The Ease Model, version 2 for windows. The Health and Safety Executive. Bootle, Merseyside, UK.

IEH (Institute of Environment and Health), 1999. Risk assessment approaches used by UK government for evaluating human health effects of chemicals. Report prepared for the Risk Assessment and Toxicology Steering Committee. The Institute for Environment and Health, Leicester, UK. ISBN 1 899110 23 2.

Inard, C., Bouia, H., Dalicieux, P., 1996. Prediction of air temperature distribution in buildings with a zonal model. Energy and Buildings 24, 125–132.

Koontz, M.D., Evans, W.C., Wilkes, C.R., 1998. Development of a model for assessing indoor exposure to air pollutants. Reported to California Air Resources Board, Research Division, Sacramento, CA 95814.

Lioy, P.J., 1990. Assessing total human exposure to contaminants. Environmental Science and Technology 24 (7), 938–945.

Maroni, M., Seifert, B., Lindvall, T. (Eds.), 1995. Indoor Air Quality. Elsevier, Amsterdam, ISBN 0-44-81642-9.

Mora, L., Gadgil, A.J., Wurtz, E., 2003a. Comparing zonal and CFD model predictions of isothermal indoor airflows to experimental data. Indoor Air 2003, V13, Part 2, pp. 77–85.

Mora, L., Gadgil A.J., Wurtz, E., Inard, C., 2003b. Comparing zonal and CFD model predictions of indoor airflows under mixed convection conditions to experimental data. Third European Conference on Energy Performance and Indoor Climate in Buildings, Lyon, France, October 23–26, 2002.

Musy, M., Wurtz, E., Nataf, J.M., 1999. An intermediate model to predict thermal comfort and air quality in a building. Indoor Air 1, 685–690.

Nielsen, P.V., 1981. Contaminant distribution in industrial areas with forced ventilation and two-dimensional flow. IIR-Joint Meeting, Commission E1, Essen, Germany.

Nielsen, P.V., 1990. Specification of a two-dimensional test case. International Energy Agency, Energy Conservation in Buildings and Community Systems, Annex 20: Air Flow Pattern Within Buildings. Department of Building Technology and Structural Engineering, Aalborg University, Denmark. ISSN 0902-7513, R9040.

NRC (National Research Council), 1983. Risk Assessment in the Federal Government: Managing the Process. Committee on the International Means for Assessment of Risks to Public Health, Commission Life Sciences, NRC. National Academy Press, Washington, DC.

NRC (National Research Council), 1990. Human Exposure Assessment for Airborne Pollutants: Advances and Applications. Committee on Advances in Assessing Human Exposure to Airborne Pollutants, Committee on Geosciences, Environment, and Resources, NRC. National Academy Press, Washington, DC.

Rajaratnam, N., 1976. Turbulent Jets. Elsevier Scientific Publishing Company, Amsterdam.

Ren, Z., 2002. Enhanced modelling of indoor air flows, temperatures, pollutant emission and dispersion by nesting sub-zones within a multi-zone model. PhD thesis, available at web site: http://www.qub.ac.uk/qc/webpages/whatwedo/researchgroups/environmentalmodelling/ia. The Queen's University of Belfast.

Ren, Z., Stewart, J., 2003. Simulating air flow and temperature distribution inside buildings using a modified version of COMIS with sub-zonal divisions. Energy and Buildings 35, 257–271.

Rodes, C.E., Kamens, R.M., Wiener, R.W., 1991. The significance and characteristics of the personal activity cloud on exposure assessment measurement for indoor contaminants. Indoor Air 2 (1), 123–145.

Rosenbaum, A., 2002. Hazardous air pollutant exposure model, version 4. The HAPEM4 User's Guide prepared for Office of Air Quality Planning and Standards, US Environmental Protection Agency, Research Triangle Park, NC.

Sparks, L.E., 1996. IAQ model for windows, RISK version 1.0, User Manual. United States Environmental Protection Agency, National Risk Management Research Laboratory, Research Triangle Park, NC, EPA-600/R-96-037.

Stewart, J., 2001. Modelling Occupational Exposure: a scoping study. QUESTOR report, The Queen's University of Belfast, UK.

Stewart, J., Ren, Z., 2003. Prediction of indoor gaseous pollutant dispersion by nesting sub-zones within a multizone model. Building and Environment 38, 635–643.

USEPA (United States Environmental Protection Agency), 1992. Guidelines for exposure assessment. U.S. Environmental Protection Agency Science Advisory Board, Washington, DC. FRL-4129-5.